AN ANALYTICAL MODEL FOR CALCULATING THE ACTIVE INTERACTION FORCES OF THE WORKING BODY OF EARTH-MOVING MACHINES WITH STICKY SOILS

Nurbol Kamzanov[1], Shynbolat Tynybekov[1], Nursat Baikenzhe[1], Guldariya Naimanova[2], Bakytzhan Kyrgyzbay[2], Rustem Kozbagarov[2,*]

[1]Satbayev University, Almaty, Republic of Kazakhstan
[2]Mukhametzhan Tynyshbayev ALT University, Almaty, Republic of Kazakhstan

*E-mail of corresponding author: r.kozbagarov@alt.edu.kz

Nurbol Kamzanov 0000-0002-2420-8362,
Nursat Baikenzhe 0009-0000-0290-9056,
Bakytzhan Kyrgyzbay 0009-0004-0317-7917,
Shynbolat Tynybekov 0009-0002-6146-2076,
Guldariya Naimanova 0000-0003-4619-7243,
Rustem Kozbagarov 0000-0002-7258-0775

Resume

In this study is presented an analytical mathematical model developed to determine the forces arising during the active penetration of machine working bodies into sticky rocks. The methodology is based on the method of element-by-element calculation of resistances, where the contact zone is divided into discrete prisms of material. As a result of the analysis, a final formula for the total penetration force is derived. This formula shows the dependence of the resistance force on the dimensions of the tool (thickness, depth, angle of sharpening) and the physical characteristics of the rock (internal friction, adhesion, stickiness). The model serves as a reliable engineering tool for the design and optimization of working bodies of earthmoving and mining equipment.

Article info

Received 31 July 2025
Accepted 30 October 2025
Online 10 November 2025

Keywords:

sticky rock
working body
earth-moving machine
angle of attack
penetration depth

Available online: https://doi.org/10.26552/com.C.2026.002

ISSN 1335-4205 (print version)
ISSN 2585-7878 (online version)

1 Introduction

The development and operation of earthmoving and mining machines, such as bulldozers, excavators, scrapers, and loaders, is inextricably linked to the problem of interaction between their working parts and the environment being processed. The efficiency, energy consumption, and service life of these machines directly depend on the resistance forces that arise during cutting, digging, and moving soil and rock [1-3]. The so-called sticky rocks pose a particular challenge for mechanized mining. These include wet clayey and loamy soils, oil-bituminous sands, and other materials with high adhesion (stickiness) to the surfaces of working bodies [4-5].

Working with sticky soils involves a number of technological difficulties [4-7]. First, high adhesive forces, combined with internal friction and cohesive forces, lead to a significant increase in overall digging resistance. This requires increased machine power, leads to fuel overconsumption, and reduces the overall productivity. Secondly, material sticking to blades, buckets, and knives distorts their working geometry, effectively "dulling" the cutting edges, which further exacerbates the first problem. Thirdly, difficulties arise with the complete unloading of buckets and bodies, which requires additional time and the use of special cleaning systems [8-9].

To solve these problems, engineers and researchers are pursuing two main approaches: developing the new materials and coatings for working parts that reduce adhesion, and optimizing the geometry of the working parts themselves. The second approach requires reliable calculation methods that allow interaction forces to be predicted at the design stage. Mathematical modelling becomes an indispensable tool in this context. It allows for a systematic study of the influence of each design parameter (e.g., cutting angle, blade thickness) on the forces that arise and finding their optimal combination [10-11].

The processes of interaction between the working bodies and material can be divided into active and passive. Passive interaction is mainly caused by the pressure of the environment on the working body

(for example, soil pressure on a blade), while active interaction is associated with the forced penetration of the working body into the mass with the supply of external energy. It is precisely the active interaction at the cutting edge of the tool that is the key and most energy-intensive process determining the cutting resistance [12-14].

The purpose of this article is to present a detailed mathematical model describing the active interaction under normal (perpendicular) impact of the working body on an array of sticky rock. This model allows us to obtain an analytical formula for calculating the penetration force, which enables design engineers to quantitatively assess the effectiveness of various design solutions.

2 Materials and methods

2.1 General approach and assumptions

The proposed mathematical model of active interaction is based on the method of element-by-element calculation of resistances. The essence of the method is that the continuous medium in the zone in front of the working body is mentally divided into several separate elements (prisms) bounded by the assumed planes of sliding. Next, the equilibrium conditions are considered for each of these prisms, which allows to construct a system of equations and find the desired forces [13-14].

The model considers two interaction options depending on the angle of the working body: with and without the formation of a compacted core in front of it. This article presents a more general case-with the presence of a compacted core, which effectively becomes an extension of the working body and changes the conditions of its interaction with the environment.

The following fundamental assumptions were made when constructing the model:

1. Prisms of material bounded by planes of slip do not compact during interaction, but move as single, “solidified” bodies. This assumption is generally accepted in classical soil cutting theories and significantly simplifies the mathematical apparatus [15-16];
2. The planes of sliding along which the material prisms shift are straight lines and emerge onto the free surface at an angle equal to the angle of internal friction of the sticky rock (φ) [15-16].

2.2 Physical model and force system

The physical model of the process is shown in Figure 1 in the source document. A working body with a thickness of a and a width of b with a sharpening angle of α is inserted to a depth of h into the sticky rock mass. A compacted core is formed in front of it, and then the mass is divided into three main sliding prisms [17-19].

Here is considered the general case of normal impact of the working body on the material surface, when the compacted core complements the working body. The equilibrium conditions of the material prisms, bounded by sliding planes, are analyzed sequentially [11, 13]:

- for a prism of material with cross-section *bdec*:

$$\begin{aligned}&\sum x = -N_3 - N_4\sin\varphi - (N_4 tg\varphi + tg\varphi K_{v2}p_2S_4)\\&\cos\psi + N_3\sin\varphi + (N_5 tg\varphi + tg\varphi K_{v2}p_2S_5)\cos\psi = 0;\\&\sum y = -N_3 tg\varphi - tg\varphi K_{v2}p_2S_3 + N_4\cos\psi -\\&-(N_4 tg\varphi + tg\varphi K_{v2}p_2S_4)\times\sin\psi - N_5\cos\psi -\\&-N_5\cos\psi + (N_5 tg\varphi + tg\varphi K_{v2}p_2S_5)\sin\psi - G_2 = 0;\end{aligned} \quad (1)$$

- for a prism of material with a cross section *bfd:*

$$\begin{aligned}&\sum x = -N_5\sin\psi - (N_5 tg\varphi + tg\varphi K_{v2}p_2S_5)\\&\cos\psi + N_6 = 0,\\&\sum y = -N_5\cos\psi - (N_5 tg\varphi + tg\varphi K_{v2}p_2S_5)\\&\sin\psi - N_6 tg\rho K_{v1} - tg\rho K_{v1}p_1S_6 - G_3 = 0;\end{aligned} \quad (2)$$

- for a prism of material with cross section *abc*:

$$\begin{aligned}&\sum x = N_1\cos\varepsilon - (N_1 tg\varphi + tg\varphi K_{v2}p_2S_1)\sin\varepsilon +\\&+N_2\cos\varepsilon + (N_2 tg\varphi + tg\varphi K_{v2}p_2S_2)\sin\varepsilon - N_3 = 0;\\&\sum y = -N_1\sin\varepsilon - (N_1 tg\varphi + tg\varphi K_{v2}p_2S_1)\cos\varepsilon +\\&+N_2\sin\varepsilon - (N_2 tg\varphi + tg\varphi K_{v2}p_2S_2)\cos\varepsilon +\\&+N_3 tg\varphi + tg\varphi K_v p_2S_3 - G_1,\end{aligned} \quad (3)$$

where N_1, N_2, N_3, N_4, N_5 and N_6, - normal reaction forces acting perpendicular to the corresponding sliding surfaces and working body surfaces; G_1, G_2 and G_3 - the gravitational forces (weight) of the corresponding soil prisms involved in the interaction; S_1, S_2, S_3, S_4, S_5, S_6 - the areas of the corresponding sliding surfaces on which the forces act; K_{v1}, K_{v2} - coefficients of the influence of speed on stickiness and adhesion indicators; φ - angle of internal friction; ψ - angle of inclination of rock slip (shear) planes relative to the horizontal; ρ - angle of external friction; p_1 - specific adhesion; p_2 - traction.

For each of the three prisms, two equilibrium equations are formulated (the sums of the projections of all the forces on the horizontal and vertical axes are zero). This leads to a system of six linear algebraic equations with six unknown reaction forces.

The values of the sliding plane area S_1, S_2, … , S_5, S_6 and the weight of the material volume G_1, G_2 and G_3 at a penetration depth h, working body thickness a, width b with a sharpening angle $2\alpha\left(\alpha \geq \frac{\pi}{4} + \frac{\varphi}{2}\right)$ are as follows:

$$S_1 = S_2 = \frac{ab}{2\sin\varepsilon}; \quad (4)$$

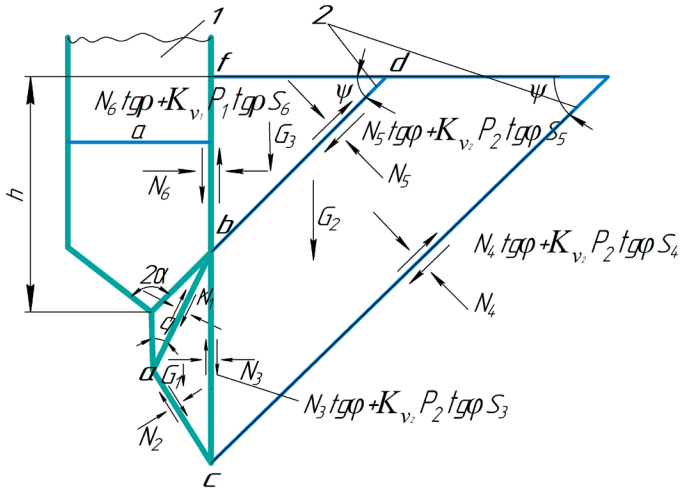

Figure 1 *Physical model of active interaction under normal impact of the working body on the rock mass: 1 - working body; 2 - sliding surface*

$$S_3 = \frac{ab}{tg\varepsilon}; \tag{5}$$

$$S_4 = \frac{a\left(h - \frac{a}{2tg\alpha} + \frac{a}{tg\varepsilon}\right)}{\sin\psi}; \tag{6}$$

$$S_5 = b\left(h - \frac{a}{2tg\alpha}\right)\frac{1}{\sin\psi}; \tag{7}$$

$$S_6 = b\left(h - \frac{a}{2tg\alpha}\right); \tag{8}$$

$$G_1 = \frac{1}{4}\frac{a^2 b}{tg\varepsilon}\gamma; \tag{9}$$

$$G_3 = \frac{1}{2}b\left(h - \frac{a}{2tg\alpha}\right)^2 ctg\psi\gamma; \tag{10}$$

$$G_2 = \frac{1}{2}bctg\psi\gamma\left[h - \left(\frac{a}{2tg\alpha} + \frac{a}{tg\varepsilon}\right)^2 - \left(h - \frac{a}{2tg\alpha}\right)^2\right] = \frac{1}{2}\gamma bctg\psi\left[\left(2h - \frac{a}{tg\alpha} + \frac{a}{tg\varepsilon}\right)\frac{a}{tg\varepsilon}\right]; \tag{11}$$

where h - depth of penetration; a - working body thickness; b - working width; α - angle of sharpening of the working body; ε - angle of the filled core; γ - material density.

2.2.1 Assumption about the shear angle

When considering the equilibrium of material prisms, bounded by the sliding planes, a relationship is established between the cutting angle of the working body α, the core filling angle ε, and the angle of inclination of the sliding planes.

In accordance with the classical principles of soil mechanics, when the compacted core acts as a continuation of the working body, the angle of inclination of the shear plane ψ to the horizon at the contact boundary is often taken according to the formula:

$$\psi = \frac{\pi}{4} + \frac{\varphi}{2}, \tag{12}$$

where φ - angle of internal friction of the material.

Since, in this general case, the compacted core complements the working body, its geometry (determined by the angle ε) directly affects the conditions for the formation of sliding planes.

The core filling angle ε is replaced by a classical expression that determines the most probable shear angle:

$$\varepsilon \approx \psi = \frac{\pi}{4} + \frac{\varphi}{2}. \tag{13}$$

This assumption allows for all the coefficients A_i to be expressed exclusively in terms of the fundamental physical properties of the material (φ, ρ) and the key geometric parameter α, which greatly simplifies engineering calculations. Further verification of the influence of this assumption is part of the required model validation.

3 Results and discussions

The main result of the work is obtaining an analytical solution for the system of equilibrium equations and deriving the final formula for calculating the insertion force of the working body.

Applying trigonometric transformations, one transforms Equations (1) - (3) and obtains an algebraic

system of equations, linear with respect to unknowns N_1 to N_6 in the form:

$$\begin{aligned}
&N_1\frac{\cos(\varepsilon+\varphi)}{\cos\varphi}+N_2\frac{\cos(\varepsilon-\varphi)}{\cos\varphi}-N_3=0;\\
&-N_1\frac{\sin(\varepsilon+\varphi)}{\cos\varphi}+N_2\frac{\sin(\varepsilon-\varphi)}{\cos\varphi}+N_3tg\varphi=\\
&K_{\upsilon 2}p_2(2S_1\cos\varepsilon-S_5)tg\varphi+G_1;\\
&N_3-N_4\frac{\sin(\psi-\varphi)}{\cos\varphi}+N_6\frac{\sin(\psi+\varphi)}{\cos\varphi}=\\
&K_{\upsilon 2}p_2(S_4-S_3)tg\varphi\cos\psi;\\
&-N_3tg+N_4\frac{\cos(\psi+\varphi)}{\cos\varphi}-N_5\frac{\cos(\psi+\varphi)}{\cos\varphi}=\\
&K_{\upsilon 2}p_2[(S_3-S_5)\sin\psi]tg\varphi+G_2;\\
&N_5\frac{\sin(\psi+\varphi)}{\cos\varphi}+N_6=K_{\upsilon 2}p_2S_5tg\varphi\cos\psi;\\
&N_5\frac{\sin(\psi+\varphi)}{\cos\varphi}-N_6=K_{\upsilon 1}p_1S_6tg\rho+\\
&+K_{\upsilon 2}p_2S_5tg\varphi\sin\psi+G_3.
\end{aligned}\tag{14}$$

The system of six Equations (14) can be conveniently divided into three independent subsystems, each containing two equations. The solution is performed sequentially, starting with the last one, which is furthest from the working body of the prism.

This system can be divided into three subsystems: I - Equations (1) and (2), II - Equations (3) and (4), III - Equations (5) and (6). Solving the subsystem III one finds the value of force N_6. To do that, one multiplies its first equation by $\cos(\psi+\varphi)$ and, adding it term by term to the second equation multiplied by $\sin(\psi+\varphi)$, one gets:

$$\begin{aligned}
&N_6[\cos(\psi+\varphi)-tg\rho\sin(\psi+\varphi)]=\\
&K_{\upsilon 2}p_2S_5tg\varphi[\cos\psi\cos(\psi+\varphi)\sin\psi+\\
&+\sin\psi\sin(\psi+\varphi)]+tg\rho K_{\upsilon 1}p_1S_6\sin\\
&(\psi+\varphi)+G_3\sin(\psi+\varphi)
\end{aligned}\tag{15}$$

or

$$N_6=K_{\upsilon 1}p_1S_6\frac{\sin\rho\sin(\psi+\varphi)}{\cos(\psi+\varphi+\rho)}+K_{\upsilon 2}p_2S_5\frac{\sin\varphi\cos\rho}{\cos(\psi+\varphi+\rho)}+G_3\frac{\cos\rho\sin(\psi+\varphi)}{\cos(\psi+\varphi+\rho)}.\tag{16}$$

From the subsystem II, one determines the value of force N_3. The first equation of the system is multiplied by $\cos(\psi+\varphi)$, and the second by $\sin(\psi+\varphi)$, and, adding them term by term, one will find:

$$\begin{aligned}
&N_3\frac{\cos(\psi+2\varphi)}{\cos\varphi}=K_{\upsilon 2}p_2tg\varphi[(S_4-S_5)\cos\varphi+\\
&+S_3\sin(\psi+\varphi)]+G_2\sin(\psi+\varphi)
\end{aligned}\tag{17}$$

or

$$\begin{aligned}
&N_3=\\
&K_{\upsilon 2}p_2\frac{[(S_4-S_5)]\cos\varphi+S_3\sin(\psi+\varphi)\sin\varphi}{\cos(\psi+2\varphi)}+\\
&+G_2\frac{\cos\varphi\sin(\psi+\varphi)}{\cos(\psi+2\varphi)}.
\end{aligned}\tag{18}$$

From system I, one determines the value of force N_1. Its first equation is multiplied by $\sin(\varepsilon-\varphi)$ and its second equation by $-\cos(\varepsilon-\varphi)$, and then, after adding them together term by term, one finds:

$$\begin{aligned}
&N_1\frac{\sin2\varepsilon}{\cos\varphi}=N_3\frac{\sin\varepsilon}{\cos\varphi}-K_{\upsilon 2}p_2(2S_1\cos\varepsilon-S_3)\\
&tg\varphi\cos(\varepsilon-\varphi)-G_1\cos(\varepsilon-\varphi)
\end{aligned}\tag{19}$$

or

$$\begin{aligned}
&N_1=N_3\frac{\sin\varepsilon}{\sin2\varepsilon}-K_{\upsilon 2}p_2(2S_1\cos\varepsilon-S_3)\\
&\frac{\sin\varphi\cos(\varepsilon-\varphi)}{\sin2\varepsilon}-G_1\frac{\cos(\varepsilon-\varphi)\cos\varphi}{\sin2\varepsilon}.
\end{aligned}\tag{20}$$

Substituting Equation (18) from (16), one calculates:

$$\begin{aligned}
&N_1=\\
&K_{\upsilon 2}p_2\frac{[(S_4-S_5\cos\varphi+S_3\sin(\psi+\varphi))\sin\psi]}{2\cos\varepsilon\cos(\psi+2\varphi)}+\\
&+G_2\frac{\cos\varphi\sin(\psi+\varphi)\cos\varphi}{2\cos\varepsilon\cos(\psi+2\varphi)}-\\
&-G_1\frac{\cos(\varepsilon+\varphi)\cos\varphi}{\sin2\varepsilon}.
\end{aligned}\tag{21}$$

The force required to drive the working body into the sticky rock mass is determined by the formula:

$$\begin{aligned}
&P_{kp}=N_1\sin\varepsilon+(N_1tg\varphi+tg\varphi K_{\upsilon 2}p_2S_1)\cos\varepsilon+\\
&+N_6tg\rho+tg\rho K_{\upsilon 1}p_1S_6
\end{aligned}\tag{22}$$

or

$$P_{kp}=N_1\frac{\sin(\varepsilon+\varphi)}{\cos\varphi}+N_6tg\rho+K_{\upsilon 1}p_1S_6tg\rho+K_{\upsilon 2}p_2S_{61}tg\varphi\cos\varepsilon.\tag{23}$$

Substituting the values of forces N_1 and N_2 into Equation (23), one obtains:

$$\begin{aligned}
&P_{kp}=\left\{K_{\upsilon 2}p_2\frac{(S_4-S_5)\cos\varphi+S_3\sin(\psi+\varphi)}{2\cos\varepsilon\cos(\psi+2\varphi)}\right.\\
&\sin\varphi+G_2\frac{\cos\varphi\sin(\psi+\varphi)}{2\cos\varepsilon\cos(\psi+2\varphi)}-\\
&\left.-G_1\frac{\cos(\varepsilon-\varphi)\cos\varphi}{\sin2\varepsilon}\right\}\times\frac{\sin(\varepsilon+\varphi)}{\cos\varphi}+\\
&+\left\{K_{\upsilon 1}p_1S_6\frac{\sin\rho\sin(\psi-\varphi)}{\cos(\psi+\varphi+\rho)}+K_{\upsilon 2}p_2S_5\right.\\
&\left.\frac{\sin\varphi\cos\rho}{\cos(\psi+\varphi+\rho)}+G_3\frac{\cos\rho\sin(\psi+\varphi)}{\cos(\psi+\varphi+\rho)}\right\}tg\rho+\\
&+K_{\upsilon 1}p_1S_6tg\rho+K_{\upsilon 1}p_1S_1tg\varphi\cos\varepsilon.
\end{aligned}\tag{24}$$

After reducing these terms and making the appropriate notations, one finds:

$$\begin{aligned}
&P_{kp}=K_{\upsilon 1}p_1b\Big(h-\frac{a}{2tg\alpha}\Big)A_1+K_{\upsilon 2}p_2\Big[\frac{ab}{2}A_2+\\
&+b\Big(h-\frac{a}{2tg\alpha}\Big)A_3\Big]-\frac{\gamma a^2b}{4}A_4+\frac{\gamma b}{2}\\
&\Big(h-\frac{a}{2tg\alpha}+\frac{a}{tg\varepsilon}\Big)^2A_5+\frac{\gamma b}{2}\Big(h-\frac{a}{2tg\alpha}\Big)^2A_6,
\end{aligned}\tag{25}$$

where

$$A_1 = \frac{\sin\rho\cos(\psi+\varphi)}{\cos(\psi+\varphi+\upsilon)} = \frac{\sin\rho\cos\left(\frac{\pi}{4}+\frac{\varphi}{2}\right)}{\cos\left(\frac{\pi}{4}+\frac{\varphi}{2}+\rho\right)}; \quad (26)$$

$$A_2 = \frac{\sin\varphi}{\sin\varepsilon}\left(\frac{\cos\varphi+\sin\varphi+\sin(\psi+\varphi)}{\sin\psi\cos(\psi+2\varphi)} + \frac{\cos\varepsilon}{\cos\varphi}\right) = \frac{3tg\varphi}{\cos\left(\frac{\pi}{4}+\frac{3}{2}\varphi\right)} + \frac{tg\varphi(1-\sin\varphi)}{\cos\varphi}; \quad (27)$$

Table 1 *The values of the coefficients A_1, A_2, A_3, A_4, A_5, A_6*

Internal friction angle φ, degree	External friction angle ρ, degree	The value of the coefficients					
		A_1	A_2	A_3	A_4	A_5	A_6
5	3	0.06	0.51	0.01	0.54	0.78	-0.64
	5	0.10	0.51	0.02	0.54	0.78	-0.60
	10	0.22	0.51	0.04	0.54	0.78	-0.45
	15	0.38	0.51	0.07	0.54	0.78	-0.26
	20	0.60	0.51	0.12	0.54	0.78	0.01
	25	0.95	0.51	0.16	0.54	0.78	0.42
	30	1.56	0.51	0.30	0.54	0.78	1.15
10	3	0.06	1.21	0.02	0.57	1.23	-0.95
	5	0.10	1.21	0.04	0.57	1.23	0.89
	10	0.22	1.21	0.09	0.57	1.23	-0.72
	15	0.39	1.21	0.17	0.57	1.23	-0.47
	20	0.64	1.21	0.27	0.57	1.23	-0.12
	25	1.05	1.21	0.44	0.57	1.23	0.46
	30	1.85	1.21	0.78	0.57	1.23	1.60
15	3	0.06	2.31	0.04	0.58	2.05	-1.48
	5	0.10	2.31	0.07	0.58	2.05	-1.41
	10	0.23	2.31	0.16	0.58	2.05	-1.10
	15	0.41	2.31	0.29	0.58	2.05	-0.87
	20	0.69	2.31	0.48	0.58	2.05	-0.40
	25	1.19	2.31	0.83	0.58	2.05	0.45
	30	2.33	2.31	1.63	0.58	2.05	2.39
20	3	0.06	4.47	0.06	0.59	3.81	-2.55
	5	0.10	4.47	0.10	0.59	3.81	-2.46
	10	0.24	4.47	0.25	0.59	3.81	-2.18
	15	0.43	4.47	0.45	0.59	3.81	-1.78
	20	0.96	4.47	0.79	0.59	3.81	-1.12
	25	1.40	4.47	1.45	0.59	3.81	0.18
	30	3.29	4.47	3.42	0.59	3.81	4.05
25	3	0.06	11.01	0.08	0.59	9.36	-5.82
	5	0.10	11.01	0.15	0.59	9.36	-5.71
	10	0.24	11.01	0.36	0.59	9.36	-5.36
	15	0.46	11.01	0.68	0.59	9.36	-4.82
	20	0.85	11.01	1.24	0.59	9.36	-3.87
	25	1.74	11.01	2.55	0.59	9.36	-1.68
	30	6.16	11.01	9.02	0.59	9.36	9.21
28	3	0.06	30.80	0.10	0.58	26.43	-15.72
	5	0.10	30.80	0.18	0.58	26.43	-15.59
	10	0.23	30.80	0.44	0.58	26.43	-15.19
	15	0.48	30.80	0.86	0.58	26.43	-14.54
	20	0.92	30.80	1.63	0.58	26.43	13.32
	25	2.06	30.80	3.49	0.58	26.43	10.11
	30	14.74	30.80	26.11	0.58	26.43	24.99

$$A_3 = \frac{\sin\varphi\sin\rho}{\sin\psi\cos(\psi+\varphi+\rho)} = \frac{\sin\varphi\sin\rho}{\cos\left(\frac{\pi}{4}+\frac{\varphi}{2}\right)\cos\left(\frac{\pi}{4}+\frac{\varphi}{2}+\rho\right)}; \quad (28)$$

$$A_4 = \frac{\cos(\varepsilon-\varphi)\sin(\varepsilon+\varphi)}{2\sin^2\varepsilon} = \frac{\sin\left(\frac{\pi}{4}+\frac{\varphi}{2}\right)\sin\left(\frac{\pi}{4}+\frac{3}{2}\varphi\right)}{1+\sin\varphi}; \quad (29)$$

$$A_5 = \frac{ctg\psi\sin(\psi+\varphi)\sin(\varepsilon+\varphi)}{2\cos\varepsilon\cos(\psi+2\varphi)} = \frac{1}{2}tg^2\left(\frac{\pi}{4}+\frac{\varphi}{2}\right)tg\left(\frac{\pi}{4}+\frac{3\varphi}{2}\right); \quad (30)$$

$$A_6 = \frac{2ctg\rho\cos\varepsilon\cos(\psi+2\varphi) - \sin(\varepsilon+\varphi)\cos(\psi+\varphi+\rho)}{2\cos\varepsilon\cos(\psi+2\varphi)\cos(\psi+\varphi+\rho)} ctg\psi\sin(\psi+\varphi) = \frac{\sin\rho\sin^2\left(\frac{\pi}{4}+\frac{\varphi}{2}\right)}{\cos\left(\frac{\pi}{4}+\frac{\varphi}{2}\right)\cos\left(\frac{\pi}{4}+\frac{\varphi}{2}+\rho\right)} - \frac{1}{2}tg^2\left(\frac{\pi}{4}+\frac{\varphi}{2}\right)tg\left(\frac{\pi}{4}+\frac{3}{2}\varphi\right), \quad (31)$$

where A_1, A_2, A_3, A_4, A_5, A_6 -are the dimensionless coefficients that depend only on the angular characteristics of the system: the angle of sharpening of the working body α, the angle of internal friction of the rock φ, and the angle of friction of the rock against the surface of the working body ρ. The formulas for calculating these coefficients are given in Equations (26)-(31) in the original work [4, 13]. The coefficients A_1 to A_6 obtained from the calculations, intended for practical use, are given in Table 1.

Table 1 shows how each coefficient changes as the external friction angle increases.

The coefficients A_1 and A_3 show a clear increase with an increase in both the internal friction angle (φ) and the external friction angle (ρ).

The coefficients A_2 and A_4 remain constant for a fixed value of φ and do not depend on the external friction angle ρ.

Coefficients A_5 and A_6 show a more complex relationship, where A_5 mainly increases, while A_6 changes its sign and also increases with increasing friction angles. This data helps to better understand the relationships between the physical properties of the material (friction angles) and the calculated coefficients.

The remaining coefficients have a more complex but analytically defined structure. Thus, the resulting formula is the final result of modelling and allows calculations of active resistance forces during the normal penetration.

3.1 Sensitivity analysis of formula P_{kp}

To assess the engineering significance of the developed model and quantitatively evaluate the influence of various input data on the final resistance force, a sensitivity analysis of the final formula P_{kp} in Equation (24) was performed.

The analysis focuses on four key parameters that have the greatest direct impact on the penetration force: h penetration depth; a working body thickness; p_1 specific adhesion; γ material density.

Sensitivity analysis was performed by sequentially varying each of the key parameters within $\pm 20\%$ of their nominal value, while the other parameters remained fixed (ceteris paribus). The change in resistance force P_{kp} during this parameter change allows to determine the sensitivity coefficient of the model to this parameter.

The analysis results show that formula P_{kp} has varying degrees of sensitivity to each of the input parameters:

- High sensitivity to geometric parameters (h and a): The force demonstrates a strong, almost linear dependence on the penetration depth and thickness of the working body. A 10% increase in h or a leads to a disproportionately greater increase of P_{kp} due to an increase in the volume of material prisms and sliding surface areas. This analytically confirms the hypothesis that optimizing the geometry of the tool is the most effective way to reduce the energy intensity of the process.
- Moderate sensitivity to adhesion p_1: The specific adhesion parameter p_1 has a significant but more predictable effect, as it directly enters the adhesion terms of Equation (24). Effect of p_1 is particularly pronounced in the case of materials with high clay and moisture content.
- Low sensitivity to density γ: Force P_{kp} is the least sensitive to the density of a material γ. This is because the members dependent on the weight of the prisms account for a smaller proportion of the total resistance force compared to the forces caused by friction and adhesion, especially at shallow penetration depths.

The data obtained allows to quantitatively assess that, to minimize the resistance force P_{kp}, the greatest engineering attention should be paid to reducing the geometric parameters and applying coatings that reduce adhesion p_1.

4 Model validation

4.1 Model limitations and justification for validation

A significant limitation of the current study is its reliance solely on the analytical derivation of the formula for determining the force of penetration P_{kp}

in Equation (24). Although the method of element-by-element calculation of resistances provides a reliable theoretical basis, the accuracy and practical applicability of the analytical expression obtained depend entirely on the simplifying assumptions made in Section 2.1 (e.g., incompressibility of prisms, straightness of the slip planes).

Therefore, the external validation is extremely important for confirming the practical reliability of the developed model.

4.2 Model validation strategy

To ensure the engineering value and reliability of the derived formula for P_{kp}, the analytical results must be quantitatively compared to the data obtained by independent methods. The following two approaches are recommended for the future work:

Experimental validation:

- Comparison of the calculated strength P_{kp} to the measured data obtained during laboratory tests (e.g., direct shear tests or miniature cutting experiments) using typical viscous or sticky soils (e.g., wet clay or loam).

This comparison should cover a range of key parameters, such as different penetration depths h, working body thickness a, and speed, to evaluate the accuracy of the model under different operating conditions

Numerical validation:

- Comparison of the calculated force P_{kp} to the results obtained by numerical methods, in particular the finite element method.

The numerical model would allow for the nonlinear behavior of the material (plasticity, compaction) and the complex geometry of the compacted core to be taken into account, providing a reliable benchmark for comparison to the simplified linear assumptions of the analytical model.

Successful validation demonstrating a close correlation between the analytical results and independent data will confirm the applicability of the model for engineering design and optimization of working bodies in sticky rock conditions. Conversely, any significant deviation would indicate the need for further refinement of the initial assumptions, especially regarding the behavior of the material under load.

5 Conclusions

In this paper is presented and described in detail a mathematical model of active interaction between the working body and an array of sticky rock during normal penetration. Based on the method of element-by-element calculation of resistances and a number of physically justified assumptions, a final analytical formula for calculating the penetration force is derived.

Key findings:

1. The developed model allows quantitative determination of resistance force as a function of the geometric parameters of the tool (thickness, width, sharpening angle) and the physical and mechanical properties of the rock (weight, friction, adhesion);
2. The formula clearly divides the total resistance into components determined by the weight of the rock, its internal strength (cohesion), and adhesive forces (adhesion), which allows for analysis of the energy expenditure structure;
3. The model analytically confirms the practical importance of optimizing the geometry of the working body, in particular, it shows the effectiveness of reducing the thickness and sharpening angle of the cutting edge to reduce the energy intensity of the cutting process.

The presented model is a ready-made engineering tool that can be used in the design of working parts for bulldozers, scrapers, excavators, and other equipment to increase their efficiency when working in difficult conditions with sticky and hard rocks. It provides a theoretical basis for making informed design decisions aimed at reducing energy consumption and increasing machine productivity.

Acknowledgements

The authors received no financial support for the research, authorship and/or publication of this article.

Conflicts of interest

The authors declare that they have no known competing financial interests or personal relationships that could have appeared to influence the work reported in this paper.

References

[1] BALOVNEV, V. I. *Modelling of interaction processes with the environment of working bodies of road construction machines*. Moscow: Higher School, 1981, ISBN 5-217-02343-0.

[2] VOLKOV, D. P., KRIKUN, V. Y., TOTOLIN, P. E., GAEVSKAYA, K. S. *Machines for earthworks.* Moscow: Mechanical Engineering, 1992. ISBN 5-217-01973-5.

[3] DOTSENKO, A. I., KARASEV, G. N., KUSTAREV, G. V., SHESTOPALOV, K. K. *Machines for earthworks.* Moscow: Bastet, 2012. ISBN 978-5-903178-28-5.

[4] BOCHAROV, V. S. *Interaction of machine tools with bitumen-containing rocks*. Moscow: Transportation, 1992. ISBN 5-277-01382-2.
[5] LUKASHUK, O. A., KOMISSAROV, A. P., LETNEV, K. Y. *Machines for soil development. Design and calculation*. Ekaterinburg: Ural University Publishing House, 2018. ISBN 978-5-7996-2386-9.
[6] FEDOROV, D. I. *Working bodies of earth-moving machines*. Moscow: Mechanical Engineering, 1977. ISBN 5-217-00490-8.
[7] DOVGYALO, V. A., BOCHKAREV, D. I. *Road construction machines. Part I: Machines for earthworks.* Gomel: Belarusian State University of Transport, 2010. ISBN 978-985-468-741-4.
[8] QING-HUA, H., DA-QING, Z., PENG, H., HAI-TAO, Z. Modelling and control of hydraulic excavator arm. *Journal of Central South University of Technology* [online]. 2006, **13**(4), p. 422-427. ISSN 1005-9784, eISSN 2227-5223. Available from: https://doi.org/10.1007/s11771-006-0061-1
[9] YANG, CH., HUANG, K., LI, Y., WANG, J., ZHOU, M. Review for development of hydraulic excavator attachment. *Energy Science and Technology* [online]. 2012, **3**(2), p. 93-97. ISSN 1923-8460, eISSN 1923-8479. Available from: https://doi.org/10.3968/j.est.1923847920120302.386
[10] KOZBAGAROV, R. A., KAMZANOV, N. S., AKHMETOVA, S. D., ZHUSSUPOV, K. A., DAINOVA, Z. K. Determination of energy consumption of high-speed rock digging. *News of the National Academy of Sciences of the Republic of Kazakhstan, Series of Geology and Technical Sciences* [online]. 2021, **6**(450), p.85-92. ISSN 2224-5278, eISSN 2518-170X. Available from: https://doi.org/10.32014/2021.2518-170X.123
[11] KOZBAGAROV, R. A., SHALBAYEV, K. K., ZHIYENKOZHAYEV, M. S., KAMZANOV, N. S., NAIMANOVA, G. T. Design of cutting elements of reusable motor graders in mining. *News of the National Academy of Sciences of the Republic of Kazakhstan, Series of Geology and Technical Sciences* [online]. 2022, **3**(453) p.128-141. ISSN 2224-5278, eISSN 2518-170X. Available from: https://doi.org/10.32014/2022.2518-170X.185
[12] GUO, Z., DU, G., LI, Z., LI, X. Orthogonal experiment on resistance reduction by soil-engaging surfaces of bulldozer blade. *Nongye Jixie Xuebao / Transactions of the Chinese Society of Agricultural Machinery* [online]. 2015, **46**(7), p. 372-378. ISSN 1000-1298. Available from: https://doi.org/10.6041/j.issn.1000-1298.2015.07.053
[13] KOZBAGAROV, R., KAMZANOV, N., AMANOVA, M. BAIKENZHEYEVA, A., NAIMANOVA, G. Justification of the cam roller parameters for destruction of the road coatings for obtaining the lumpy asphalt scrap. *Communications - Scientific Letters of the University of Zilina* [online]. 2023, **25**(2), p. 103-1097. ISSN 2585-7878, eISSN 1335-4205. Available from: https://doi.org/10.26552/com.C.2023.028
[14] KOZBAGAROV, R. A., ZHIYENKOZHAYEV, M. S., KAMZANOV, N. S., TSYGANKOV, S. G., BAIKENZHEYEVA, A. S. Design of hydraulic excavator working members for development of mudslides. *News of the National Academy of Sciences of the Republic of Kazakhstan, Series of Geology and Technical Sciences* [online]. 2023, **2**(458), p. 134-141. ISSN 2224-5278, eISSN 2518-170X. Available from: https://doi.org/10.32014/2023.2518-170X.288
[15] TROYANOVSKAYA, I., GREBENSHCHIKOVA, O. Optimization of technical productivity of a bulldozer unit in terms of traction and speed parameter. *The Russian Automobile and Highway Industry Journal* [online]. 2025, **21**(6), p. 844-851. ISSN 2071-7296, eISSN 2658-5626. Available from: https://doi.org/10.26518/2071-7296-2024-21-6-844-8517
[16] MIAO, CH. Modeling and simulation research on the hydraulic system of the blade of an unmanned bulldozer. *Frontiers in Computing and Intelligent Systems* [online]. 2025, **11**(2), p.78-82. ISSN 2832-6024. Available from: https://doi.org/10.54097/n8pphn83
[17] YULIUS, M., NURBAITI, SARMIDI, MUHAMMAD, I. G. Usage procedure of Liebherr 756 bulldozer unit in live stockpile OPB 4 PT Bukit Asam Tbk/Prosedur penggunaan unit bulldozer Liebherr 756 di live stockpile OPB 4 PT. Bukit Asam, Tbk (in Indonesian). *Scientific Journal of Engineering and Science* [online]. 2025, **2**(1), p. 117-123. eISSN 3025-8871. Available from: https://doi.org/10.62278/jits.v2i1.50
[18] SHARMA, D., BARAKAT, N. Evolutionary bi-objective optimization for bulldozer and its blade in soil cutting. *Journal of The Institution of Engineers (India): Series C* [online]. 2019, **100**(2), p. 295-310. ISSN 2250-0545, eISSN 2250-0553. Available from: https://doi.org/10.1007/s40032-017-0437-z
[19] AKANKSHA, M., VIKAS, K. S., SHIVAM, VIPUL, C. A comprehensive review of bulldozers in modern construction. *Journal of Scientific Research and Reports* [online]. 2024, **30**(5), p. 337-342. ISSN 2320-0227. Available from: https://doi.org/10.9734/JSRR/2024/v30i51949